Decay Model for Dispersion of Coastal Discharged Effluents from Multiport Diffusers in the Far-field

Anton Purnama[1], Huda A. Al-Maamari[2], E. Balakrishnan[3]
[1,2,3]*Department of Mathematics, College of Science, Sultan Qaboos University, Muscat, Sultanate of Oman*

Abstract– Ocean disposal of pretreated urban wastewater and desalination brine effluents through multiport diffusers is a safe, economical and reliable disposing scheme for coastal industrial plants. These reactive effluents might include pollutants with different loss rates that varies with water depth. A mathematical modeling study is presented to evaluate the effect of a step change in water depth upon spreading of coastal discharged of effluents in the far-field using a two-dimensional decay-advection-diffusion equation with multiple point sources. Analytical solutions are illustrated graphically by plotting contours of concentration to replicate the spreading of discharged effluent plumes in the coastal waters. The diffuser-compounded concentration at the shoreline is formulated to account for the variability of decay of discharged effluents with water depth and its maximum value is used as a measure for assessing the water quality standards in coastal marine environment.
Keywords – Decay-advection-diffusion equation; environmental impact assessment; method of image; sea outfall; shoreline concentration; step seabed

I. INTRODUCTION

An outfall is a long pipeline which terminates in a diffuser and is used for discharging large amounts of municipal (treated) wastewaters, cooling waters, or desalination brine effluents into the open sea [1-5]. Coastal discharged effluents contain some unknown reactive chemicals that are subject to significant (temporal) decay. The (physical, chemical and biological) decay processes include consumption by bacteria, heat loss or evaporation through the surface, and break up or dissolution by turbulence. A multiport diffuser is a linear structure consisting of many closely spaced ports to release a series of effluent streams [6,7]. The environmental effects of discharging effluents wastewater through a well-designed long outfall system are reported to be minimal, as it apparently prevents the discharged effluent plumes from reaching coastal areas, thereby protecting the public health for using beaches for swimming and other recreational purposes [1,2,5,8]. One factor affecting the dispersion of discharged wastewater effluents is the seabed depth profiles [9-11], which typically range between a sloping sandy beach and a mountainous coast with rocky coastal cliffs with steep slopes descending into the sea, where the water depth gets very deep within a short distance from the coastline. However, since the coastal area is a dynamic region where land and sea meet, the sandy beaches are actively adjusting their form to an equilibrium profile in response to erosion [12-15]. In the oceanography textbooks, going further seaward from the shore, the first submerged region is termed continental shelf. The seaward limits of the shelf are set by the distinct change in depths between the shelf and its adjacent continental slope. Thus, a seabed depth profile is typically depicted as a shallow depth coming in contact with a deeper one.

Due to the unpredictable sea conditions, mathematical modeling has been widely used to demonstrate the effectiveness of an outfall for discharging effluents into the coastal waters [16-19]. For calm sea conditions, the time scales for transverse mixing can be of order a day and comparable with the time scales for discharged effluents decay. So, the effects of decay can not be regarded as a minor perturbation that simply lower the concentration level. While the far field models involve drastic simplifications, key physical mixing and dispersion processes are represented, and thus the analytical solution remains useful in providing a qualitative understanding and in suggesting general spreading of the discharged effluent plumes in the coastal waters. The variability of decay with water depth is investigated using a two-dimensional decay-advection-diffusion equation with multiple point sources on a step seabed, and the maximum value of concentration at the shoreline will be formulated and used as an environmental standard measure for how well the discharged effluent plumes are diluted in coastal waters.

We introduce a step seabed depth profile (Figure 1 (left)), where the sudden water depth change occurs only across the line $y = \ell h_0$ (parallel to the straight shoreline at $y = 0$). h_0 is the shallow water depth in the (finite) nearshore region $0 \le y < \ell h_0$ and h_1 the deeper water depth in the (semi-infinite) offshore region $y > \ell h_0$, where $r = h_1/h_0$ is the ratio of water depths across the discontinuity line $y = \ell h_0$. Note that if $r = 1$, there is no depth changes, and this simple depth profile is known as a flat seabed.

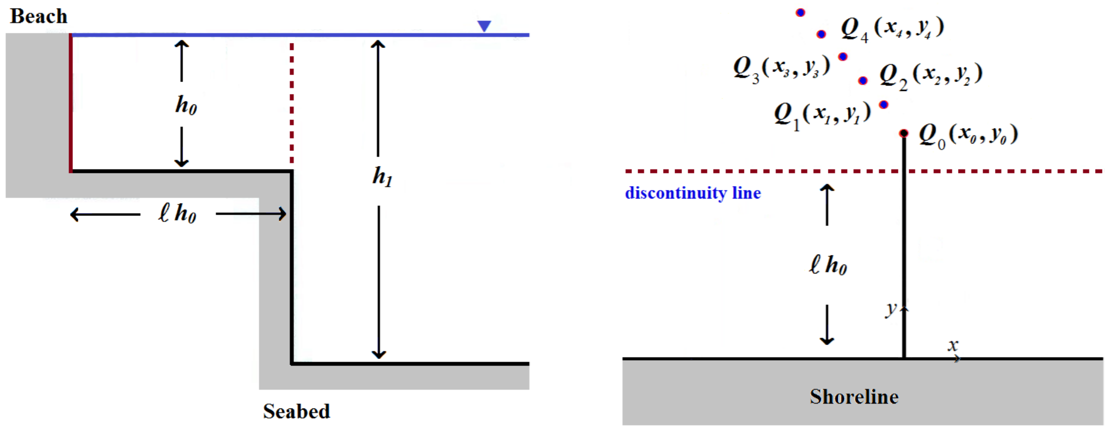

Figure 1 Cross-section depth profile of a step seabed (left); and diagram of multiple point sources representing a multiport diffuser (right)

The coastline is considered to be straight and the sea wide, and the outfall's discharged effluent plumes in the far-field is assumed to be vertically well-mixed over the water depth. Without loss of generality, we represent the first port (single outfall) discharging an effluent stream at a rate Q_0 as a point source at the end of the outfall pipeline $(x_0 = 0, y_0 = \alpha h_0)$. As shown in Figure 1 (right), for a multiport diffuser with *N*-ports (in addition to the single outfall), the second port discharging at a rate Q_1 is represented as a point source located at $(x_1 = -ph_0, y_1 = (\alpha + d)h_0)$; the third port discharging at a rate Q_2 as a point source at $(x_2 = -2ph_0, y_2 = (\alpha + 2d)h_0)$; and so on, where ph_0 is the port's (offshore) and dh_0 (along the shore) separation distances. Both values of *p* and *d* are small compared to the single outfall pipe length α. We represent the kth-port discharging at a rate Q_k by a point source at (x_k, y_k), where $x_k = -kp\,h_0$, $y_k = (\alpha + kd)h_0$ with $k = 0,1,2,\cdots,N$. Note that, if the total effluent load *Q* is distributed equally and discharged through a multiport diffuser with $N+1$ ports, each port discharges at a rate of $Q_k = Q/(N+1)$, and for a single outfall ($k = 0$), $Q_0 = Q$. That is, Q usually takes the value of the original discharge rate of the first (single) outfall.

The longshore (drift) current in the shallow nearshore region is assumed to be steady with speed U_0 and remain in the *x*-direction (positive to the right of the single outfall). The dispersion processes are represented by eddy diffusivities D_0, and diffusion in the *x*-direction is neglected, as the effluent plumes in steady currents become very elongated in the direction parallel to the shoreline. The (first-reaction) temporal decay rate is represented by μ_0, with a typical value up to 0.5 day^{-1} for decay of faecal bacteria in recreation coastal waters [5,20], decay of dissolved oil (biological consumption of hydrocarbons) [21], and decay of biological oxygen demand [22]. In the deeper offshore region, we model both the current U_1 and coefficient of dispersivity D_1 as the power functions of water depth, where U_1 is proportional to $h_1^{1/2}$ and D_1 to $h_1^{3/2}$. These scaling are appropriate for a turbulent shallow-water flow over a smooth bed [23,24]. We also assume that the loss rate of discharged effluents μ_1 as a function of water depth and proportional to $h_1^{1/2+\sigma}$, where σ represents the variability of decay with water depth [25,26]. In the far-field modeling [9-11,16,17], the other complexities such as tidal motions, density and temperature are ignored.

On writing the effluent concentration as

$$c(x, y) = \begin{cases} c^*_-(x, y), & 0 \le y < \ell h_0 \\ c^*_+(x, y), & y > \ell h_0 \end{cases},$$

the analytical solution of the decay-advection-diffusion equation with multiple point sources discharging on a step seabed can be obtained using the method of image, where the depth discontinuity at the line $y = \ell h_0$ will be considered as a reflecting or absorbing barrier. For example, as illustrated in Figure 2 (left) where the solid lines are in fact rays [10,11], for a point source located in the deeper offshore region, an observer there will supposedly see this actual source plus its own image source on the other side of the reflecting barrier at $y = \ell h_0$. However, for an observer in the shallow nearshore region, he or she will see one associated virtual (instead of the actual) source over the absorbing barrier at $y = \ell h_0$. Similarly, for a point source located in the shallow nearshore region (Figure 2 (right)), an observer there will supposedly see this actual source plus its own image source on the other side of the reflecting barrier at $y = \ell h_0$. However, for an observer in the deeper offshore region, he or she will see one associated virtual (instead of the actual) source over the absorbing barrier at $y = \ell h_0$.

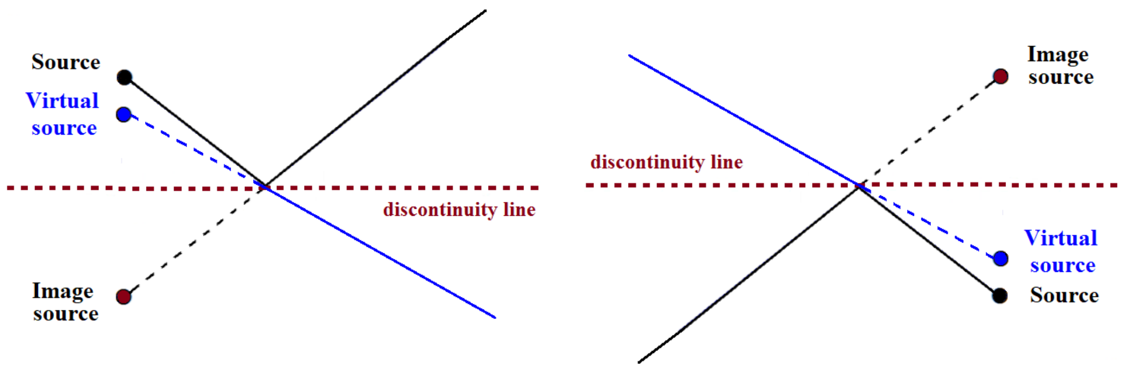

Figure 2 Diagram of the positions of the (actual) source, image source, and virtual source used in the method of image

The paper is structured as follows. A mathematical model formulation for discharged effluents from multiple point sources on a step seabed are presented in section II. The results and discussions on the solution obtained for a single outfall are given in section III, for a two-port diffuser in section IV, and for a multiport diffuser in section V. Some concluding remarks are provided in section VI.

II. DECAY-ADVECTION-DIFFUSION EQUATION WITH MULTIPLE POINT SOURCES

We consider a point source at (x_k, y_k) in the deeper offshore region $y > \ell h_0$ (Figure 1 (right)) that represents the location of the kth-port in a multiport diffuser. By treating the discontinuity line $y = \ell h_0$ as an absorbing barrier, the discharged effluents concentration $c^*_{k-}(x,y)$ in the shallow nearshore region $0 \le y < \ell h_0$ is obtained from a virtual (point) source at $(x = -kph_0, y = \beta_k h_0)$ discharging with a rate bQ_k. By applying the superposition principle $c^*_{-}(x,y) = \sum_{k=0}^{N} c^*_{k-}(x,y)$, the two-dimensional decay-advection-diffusion equation for $c^*_{k-}(x,y)$ can be written as

$$h_0 \mu_0 c^*_{k-} + h_0 U_0 \frac{\partial c^*_{k-}}{\partial x} - h_0 D_0 \frac{\partial^2 c^*_{k-}}{\partial y^2} = bQ_k\, \delta(x + kph_0)\,\delta(y - \beta_k h_0),$$

with the boundary condition $h_0 D_0\, \partial c^*_{k-} / \partial y = 0$ at the shoreline $y = 0$, and $\delta(*)$ is the Dirac delta function which represents the position of a virtual source. The temporal decay term can be eliminated from the equation by re-writing $c^*_{k-} = c_{k-} \exp\{-\mu_0 (x + kph_0)/U_0\}$. Note that the concentration of discharged effluents at the shoreline can be adjusted by varying the outfall's length. Thus, for sufficiently long outfall, the boundary condition at the shoreline is conveniently satisfied.
We define dimensionless quantities

$$c_k\left(x,y\right)=\frac{C_k\left(X,Y\right)Q}{h_0{}^2U_0},\ x=Xh_0,\ y=Yh_0,\ \lambda=\frac{U_0h_0}{D_0}\ \text{and}\ \gamma=\frac{\mu_0h_0}{U_0}.$$

Thus, in dimensionless form $C^*{}_{k-}=C_{k-}\exp\left\{-\gamma\left(X+kp\right)\right\}$ and the equation is reduced to

$$\frac{\partial C_{k-}}{\partial X}-\frac{1}{\lambda}\frac{\partial^2C_{k-}}{\partial Y^2}=bq_k\ \delta\left(X+kp\right)\delta\left(Y-\beta_k\right)$$

and for $X\geq -pN$, the analytical solution is given by, after summing for all concentrations C_{k-} from the kth-port,

$$C_-\left(X,Y\right)=\sum_{k=0}^{N}C_{k-}\exp\left\{-\gamma\left(X+kp\right)\right\}=\sum_{k=0}^{N}bq_k\sqrt{\frac{\lambda}{4\pi\left(X+kp\right)}}\exp\left\{-\frac{\lambda\left(Y-\beta_k\right)^2}{4\left(X+kp\right)}-\gamma\left(X+kp\right)\right\},\qquad(1)$$

where $q_0=Q_0/Q$, $q_k=Q_k/Q$ and $\sum_{k=0}^{N}q_k=1$. The model parameter λ represents the effluent plume elongation in the x-direction. The larger the values of λ, the more elongated the plumes are, which is mostly due to a stronger current U_0 with less longitudinal dispersivity D_0. However, the larger values of γ are mostly due to a stronger decay μ_0 with calm sea conditions U_0. The decay rate is naturally small, and in order for the effects of decay to be noticeable, a sufficiently large values of γ should be considered. For model applications in coastal waters, appropriate values are $\lambda=0.2$ and $\gamma=0.0005$.

In the deeper offshore region $y>\ell h_0$, the discontinuity line $y=\ell h_0$ is treated as a reflecting barrier, and the discharged effluents concentration $c^*{}_+\left(x,y\right)$ is obtained due to the kth-point (actual) source at $\left(x_k,y_k\right)$ discharging with a rate Q_k and due to an image source at $\left(x=-kph_0,y=\left(2\ell-\alpha-k\,d\right)h_0\right)$ discharging with a different rate aQ_k. Thus, by applying the superposition principle $c^*{}_+\left(x,y\right)=\sum_{k=0}^{N}c^*{}_{k+}\left(x,y\right)$, the decay-advection-diffusion equation for $c^*{}_{k+}\left(x,y\right)$ can be written as

$$h_1\mu_1c^*{}_{k+}+h_1U_1\frac{\partial c^*{}_{k+}}{\partial x}-h_1D_1\frac{\partial^2c^*{}_{k+}}{\partial y^2}=Q_k\delta\left(x+kph_0\right)\left[\delta\left(y-\left(\alpha+k\,d\right)h_0\right)+a\,\delta\left(y-2\ell h_0+\left(\alpha+k\,d\right)h_0\right)\right],$$

with the condition $c^*{}_{k+}\left(x,y\right)\to 0$ as $y\to\infty$, i.e. the discharged effluents concentration is ultimately diluted at a far distance. Eliminating the decay term by re-writing $c^*{}_{k+}=c_{k+}\exp\left\{-\mu_1\left(x+kph_0\right)/U_1\right\}$, where $U_1=U_0r^{1/2}$, $D_1=D_0r^{3/2}$ and $\mu_1=\mu_0r^{1/2+\sigma}$. In dimensionless form $C^*{}_+\left(x,y\right)=C_{k+}\exp\left\{-\gamma r^{\sigma}\left(X+kp\right)\right\}$, the equation becomes

$$\frac{\partial C_{k+}}{\partial X}-\frac{r}{\lambda}\frac{\partial^2C_{k+}}{\partial Y^2}=\frac{1}{r^{3/2}}q_k\delta\left(X+kp\right)\left[\delta\left(Y-\alpha-k\,d\right)+a\delta\left(Y-2\ell+\alpha+k\,d\right)\right].$$

Again, we obtain the solution, after summing for all N-ports,

$$\begin{aligned}C_+\left(X,Y\right)&=\sum_{k=0}^{N}C_{k+}\exp\left\{-\gamma r^{\sigma}\left(X+kp\right)\right\}\\&=\sum_{k=0}^{N}\frac{q_k}{r^2}\sqrt{\frac{\lambda}{4\pi\left(X+kp\right)}}\exp\left\{-\gamma r^{\sigma}\left(X+kp\right)\right\}\times\\&\qquad\left[\exp\left\{-\frac{\lambda\left(Y-\alpha-k\,d\right)^2}{4r\left(X+kp\right)}\right\}+a\exp\left\{-\frac{\lambda\left(Y-2\ell+\alpha+k\,d\right)^2}{4r\left(X+kp\right)}\right\}\right]\end{aligned}\qquad(2)$$

As there can be no sharp discontinuities in either the concentration or its gradient across the discontinuity line $y=\ell h_0$, the additional matching conditions [11]:

$$\lim_{y\to \ell h_0} c^*_{k-} = \lim_{y\to \ell h_0} c^*_{k+} \quad \text{and} \quad \lim_{y\to \ell h_0} h_0 D_0 \frac{\partial c^*_{k-}}{\partial y} = \lim_{y\to \ell h_0} h_1 D_1 \frac{\partial c^*_{k+}}{\partial y}$$

are required for calculating the coefficients *a*, *b* and β_k. After some manipulations and simplifications, we obtain

$$a = \frac{r^2-1}{r^2+1},\ b\exp\{-\gamma(X+kp)\} = \frac{2}{r^2+1}\exp\{-\gamma r^{\sigma}(X+kp)\},\ \beta_0 = \frac{\alpha-\ell}{\sqrt{r}}+\ell \ \text{and}\ \beta_k = \beta_0 + \frac{kd}{\sqrt{r}}.$$

For no decay ($\gamma = 0$) discharged effluents, it is easy to verify $a+b=1$ and if there is no depth change across the line $y = \ell h_0$, i.e. $r=1$, then $a=0$, $b=1$, $\beta_0 = \alpha$ and $\beta_k = \alpha + kd$. Note also that if $\ell = 0$ (i.e., no depth discontinuity), then $r=1$.

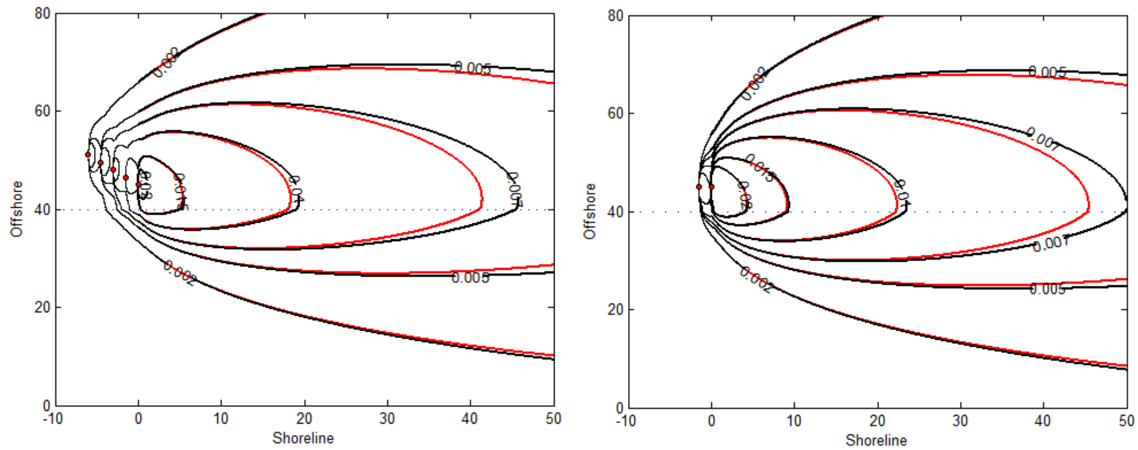

Figure 3 Contours of solutions for effluents discharge at $\alpha = 45$ with $\lambda = 0.2$ on a step seabed when $\ell = 40$ and $r = 2$ for: five points source with $d = p = 1.5$ (left); and two points source with $d = 1.5$, $p = 0$ (right). The case of no decay $\gamma = 0$ (black contour) and decay of $\gamma = 0.0005$ that increases with depth $\sigma = 1$ (red contour)

Figure 3 (left) illustrates graphically the contours of solutions for five point sources at $\alpha = 45$ with $\lambda = 0.2$, where each point is discharging at equal rate of $q_k = 1/5$ on a step seabed depth when $\ell = 40$ and $r = 2$. As observed in coastal waters, the actual discharged effluent plumes are elongated in the *x*-direction, and the larger values of λ will spread the plumes over large downstream distances [18,19]. The merging of discharged plumes is evident, and downstream of the first point (i.e., $X \ge 0$), the combined plumes is spreading like one, which supports the concept that a multiport diffuser will rapidly dilute the effluents discharged in coastal waters. The case of no decay ($\gamma = 0$) of discharged effluents is plotted by black curve, and decay at a rate of $\gamma = 0.0005$ that increases with depth $\sigma = 1$ by red curve. Due to loss of discharged effluents, the plumes of $\gamma = 0.0005$ are smaller than that of no decay $\gamma = 0$ plumes. For comparison, the contours of solution for two point source, where each point is discharging at an equal rate of $q_0 = q_1 = 1/2$ is also shown in Figure 3 (right). These contours replicate the discharged effluent plumes from a two-port diffuser spreading towards the shoreline in the far field.

The main objective of sea outfall's discharge is to prevent the discharged effluent plumes from reaching coastal areas of human usage. A typical standard regulatory criterion would state "does not exceed a certain prescribed level of concentration anywhere along the beach" to control public health risks where coastal waters are used for recreational purposes. Thus, the maximum value of concentration at the shoreline can be used as an appropriate measure for assessing the potential impact of coastal discharged effluents into the sea [11,18,19]. Substituting $Y = 0$, we obtain the concentration of discharged effluents at the shoreline

$$C_-(X,0) = \frac{1}{r^2+1}\sum_{k=0}^{N} q_k \sqrt{\frac{\lambda}{4\pi(X+kp)}}\exp\left\{-\frac{\lambda\beta_k^2}{4(X+kp)} - \gamma r^{\sigma}(X+kp)\right\}. \tag{3}$$

The effects of loss of discharged effluents that varies with water depth will be investigated according to the values of σ, and for model application, the values of $\gamma = 0$ (no decay), $\gamma = 0.0005$ and $\sigma = 0$ (constant rate), and $\gamma = 0.0005$ and $\sigma = 1$ for decay rate that increases with water depth.

III. DISCHARGE FROM A SINGLE (PORT) OUTFALL

For model applications, we first consider the simplest case of a sea outfall pipeline that terminates in a single port. The results will be used and served as the base value for the effectiveness of multiport diffusers. Since the total effluents load is released through this outfall that ends at $(x_0 = 0, y_0 = \alpha h_0)$, in this case, $q_0 = 1$.

The solution in the shallow nearshore region $0 \le y < \ell h_0$ for a single outfall's discharged effluents is obtained from (1) by setting $k = 0$, that is

$$C_{0-}(X,Y) = \frac{2}{r^2+1}\exp\left(-\gamma r^{\sigma} X\right)\sqrt{\frac{\lambda}{4\pi X}}\exp\left\{-\frac{\lambda(Y-\beta_0)^2}{4X}\right\}$$

and in the deeper offshore region $y > \ell h_0$ from (2),

$$C_{0+}(X,Y) = \frac{1}{r^2}\exp\left(-\gamma r^{\sigma} X\right)\sqrt{\frac{\lambda}{4\pi X}}\left[\exp\left\{-\frac{\lambda(Y-\alpha)^2}{4rX}\right\} + a\exp\left\{-\frac{\lambda(Y-2\ell+\alpha)^2}{4rX}\right\}\right].$$

The contour plot of the solutions for discharged effluents from a point source at $\alpha = 45$ with $\lambda = 0.2$ on a step seabed when $\ell = 40$ and $r = 2$ is shown in Figure 4 (left). The case of no decay ($\gamma = 0$) discharged effluents is plotted by black contours, constant decay of $\gamma = 0.0005$ and $\sigma = 0$ by blue contours, and decay of $\gamma = 0.0005$ that increases with depth by red contours. The contours illustrate that since decay rate is naturally small, in order for the effects of decay to be noticeable, a sufficiently large values of γ should be considered.

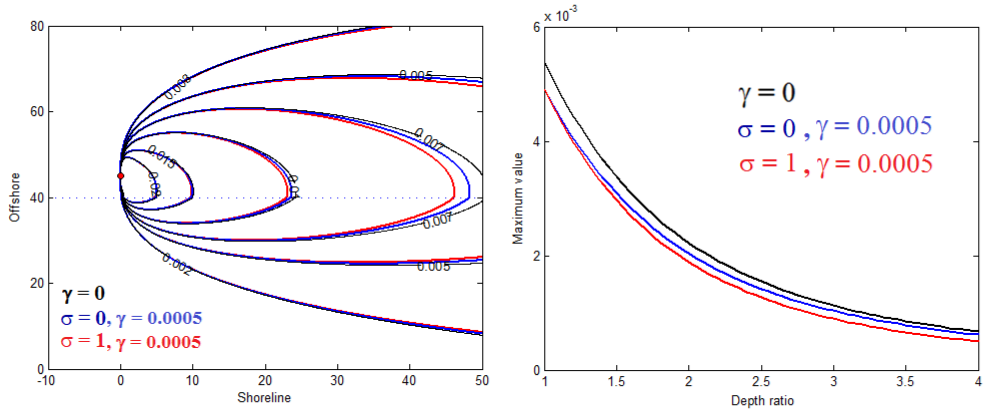

Figure 4 Contours of solutions for effluents discharge from a point source at $\alpha = 45$ with $\lambda = 0.2$ on a step seabed when $\ell = 40$ and $r = 2$ (left); and the maximum value C_{0m} of concentration at the shoreline (right). The case of no decay $\gamma = 0$ (black contour), constant decay of $\gamma = 0.0005$ and $\sigma = 0$ (blue contour), and decay of $\gamma = 0.0005$ that increases with depth $\sigma = 1$ (red contour)

Substituting $Y = 0$, we obtain from (3) for $X \ge 0$, the concentration of discharged effluents at the shoreline

$$C_{0-}(X,0) = \frac{2}{1+r^2}\sqrt{\frac{\lambda}{4\pi X}}\exp\left(-\frac{\lambda\beta_0^{\,2}}{4X} - \gamma r^{\sigma} X\right),$$

and by differentiating, it has a maximum value of

$$C_{0m} = \frac{2}{r^2+1}\sqrt{\frac{1}{2\pi\beta_0^{\,2}\Phi}}\exp\left(-\frac{2-\Phi}{2\Phi}\right),$$

which occurs at $X_{0m} = \lambda\beta_0^{\,2}\Phi/2$ where $\Phi = 2\Big/1+\sqrt{1+4\gamma r^{\sigma}\lambda\beta_0^{\,2}}$.

This maximum value C_{0m} will be used as the (reference) base value for the design effectiveness of marine outfall systems. For no decay ($\gamma = 0$) discharged effluents, then $\Phi = 1$,

$$C_{0m} = \frac{2}{r^2+1}\sqrt{\frac{1}{2\pi\beta_0{}^2 e}} \text{ and } X_{0m} = \frac{\lambda\beta_0{}^2}{2}.$$

It is straightforward to check that for the case of a flat seabed (i.e., no depth change) $r=1$, the maximum value reduces to $\left(1/\beta_0\right)\sqrt{1/2\pi e}$ [11].

As plotted in Figure 4 (right) the maximum value C_{0m} decreases significantly as the depth ratio r increases. As given in Table 1 for the case of no decay ($\gamma=0$) discharged effluents from a point source at $\alpha=45$, the maximum value on a step seabed with $r=1.5$ is about 37% lower than that of the flat seabed ($r=1$). However, if the water depth in the shallow nearshore region is only half of that in the deeper region (i.e., $r=2$), the maximum value is about 59% lower than that of a flat seabed. Moreover, the offshore distance ℓ of the discontinuity line has little effect on the maximum value C_{0m}. Thus, unless stated otherwise, the value of $\ell=40$ is used in the subsequent calculations and plots.

Table -1 Maximum values C_{0m} for discharging no decay ($\gamma=0$) effluents

	$\ell=34$	$\ell=36$	$\ell=38$	$\ell=40$	$\ell=42$	$\ell=44$
$r=1$	0.0054	0.0054	0.0054	0.0054	0.0054	0.0054
$r=1.5$	0.0035	0.0034	0.0034	0.0034	0.0033	0.0033
$r=2$	0.0023	0.0023	0.0023	0.0022	0.0022	0.0022
$r=2.5$	0.0016	0.0016	0.0016	0.0015	0.0015	0.0015
$r=3$	0.0012	0.0012	0.0012	0.0011	0.0011	0.0011

IV. DISCHARGE FROM A TWO-PORT DIFFUSER

We consider the case of a sea outfall pipeline that terminates in a two ports. Since the total effluents load is released through these two ports, in this case we have $q_0+q_1=1$.

The solution in the shallow nearshore region $0 \le y < \ell h_0$ for a two-port diffuser discharging is obtained from (1) by setting $k=1$, i.e. $C_-\left(X,Y\right)=C_{0-}\exp\left(-\gamma X\right)+C_{1-}\exp\left\{-\gamma\left(X+p\right)\right\}$. To calculate the maximum value of the compounded concentration of discharged effluents at the shoreline, we substitute $Y=0$ and obtain from (3) for $X \ge -p$,

$$C_-\left(X,0\right)=C_{0-}\left(X,0\right)\left[q_0+q_1\sqrt{\frac{X}{X+p}}\exp\left\{-\frac{\lambda\beta_1{}^2}{4\left(X+p\right)}+\frac{\lambda\beta_0{}^2}{4X}-\gamma r^{\sigma}p\right\}\right],$$

where $C_{0-}\left(X,0\right)$ is the single outfall's concentration at the shoreline.

To investigate the effect of effluents decay, the compounded concentration at the shoreline for two point sources at $\alpha=45$ with $d=p=1.5$ on a step seabed when $\ell=40$ and $r=2$ is plotted in Figure 5 (left) where each point is discharging at an equal rate of $q_0=q_1=1/2$ and $\lambda=0.2$. For comparison, the concentration at the shoreline for a single outfall at $\alpha=45$ discharging with a rate $q_0+q_1=1$ is also shown with a dotted black curve. The case of constant decay of $\gamma=0.0005$ and $\sigma=0$ is plotted by blue curve, and decay of $\gamma=0.0005$ that increases with depth $\sigma=1$ by red curve. As expected due to loss of discharged effluents, the compounded concentrations at the shoreline for $\gamma=0.0005$ are smaller than that of no decay ($\gamma=0$).

Next, on substituting $X=X_{0m}$, the maximum value can be approximated as

$$\frac{C_{1m}}{C_{0m}}=q_0+q_1\exp\left(-\gamma r^{\sigma}p\right)\sqrt{\frac{1}{1+z}}\exp\left[-\frac{1}{2\Phi}\left\{\left(\frac{\beta_1}{\beta_0}\right)^2\frac{1}{1+z}-1\right\}\right]$$

where $z=2p/\lambda\beta_0{}^2\Phi$. Since the value of γ is naturally small, $\beta_1=\beta_0+d/\sqrt{r}$, and the port's separation distances are relatively small, we obtain asymptotically

$$\frac{C_{1m}}{C_{0m}}=1-\frac{q_1}{\Phi}\frac{d}{\beta_0\sqrt{r}}\left\{1+\left(\frac{\Phi-1}{2\Phi}\right)\frac{d}{\beta_0\sqrt{r}}-\frac{3}{2}z\right\}-q_1\frac{z}{2\Phi}\left\{\Phi-1+\left(\frac{3}{2}-\frac{3\Phi}{4}-\frac{1}{4\Phi}\right)z\right\}+\cdots,$$

Thus, the maximum value of the compounded concentration of discharged effluents at the shoreline from a two-port diffuser C_{1m} is less than that of the single outfall's C_{0m}. Note that for the case of decay ($\gamma=0$) effluents, then $\Phi=1$ and

$$\frac{C_{1m}}{C_{0m}}=1-q_1\left[\frac{d}{\beta_0\sqrt{r}}\left\{1-3\left(\frac{p}{\lambda\beta_0^{\,2}}\right)\right\}+\left(\frac{p}{\lambda\beta_0^{\,2}}\right)^2\right]+\cdots.$$

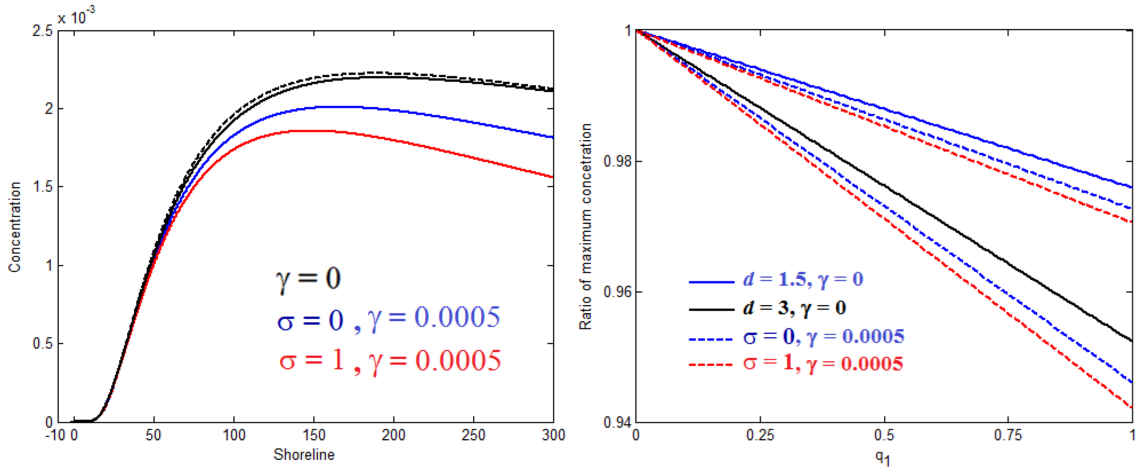

Figure 5 Compounded concentration at the shoreline for effluents discharge from two point sources at $\alpha=45$ with $d=p=1.5$ for $\lambda=0.2$ on a step seabed when $\ell=40$ and $r=2$ (left); and the ratio of maximum values C_{1m}/C_{0m} (right) for the case of no decay $\gamma=0$ with $d=1.5$ (blue line) and with $d=3$ (black line), constant decay of $\gamma=0.0005$ and $\sigma=0$ (dotted blue line), and decay of $\gamma=0.0005$ that increases with depth $\sigma=1$ (dotted red line)

As shown on Figure 5 (right), as the discharge rate q_1 increases and d gets longer, the maximum value C_{1m} is smaller than that of the first outfall C_{0m}. This result agrees with the finding that the total effluent load can be optimally allocated between two ports to minimize the impact [19,27,28]. However, since the value of γ is naturally small, the effect of decay is too small to be noticeable. Since $z=p/\lambda\beta_0^{\,2}=0.004$ (for $p=1.5$ when $\alpha=45$, $\ell=40$ and $r=2$) is small, the variability of decay of discharged effluents with water depth has a very little effect on the maximum value C_{1m}. For example, for no decay ($\gamma=0$) effluent discharges, if $d/\beta_0\sqrt{r}=0.049$ (for $d=3$ when $\alpha=45$, $\ell=40$ and $r=2$) and $z=p/\lambda\beta_0^{\,2}=0.004$ (for $p=1.5$) discharging at an equal rate $q_0=q_1=0.5$, then the maximum value C_{1m} is about 2.4% less than C_{0m}. However, this reduction increases to 6% for the case of effluents decay of $\gamma=0.0005$ that increases with depth $\sigma=1$.

Note that for a special design where the two-port line diffuser is placed in the *y*-axis perpendicular to the current direction (see Figure 6 (left)), i.e. $p=0$ or $z=0$, and each port is discharging at an equal rate of $q_0=q_1=1/2$, then

$$\frac{C_{1m}}{C_{0m}}=1-\frac{d}{\beta_0\sqrt{r}}\left\{\frac{1}{2\Phi}+\left(\frac{\Phi-1}{4\Phi^2}\right)\frac{d}{\beta_0\sqrt{r}}\right\}+\cdots.$$

Similarly, when the two-port line diffuser is placed in the x-axis parallel to the current direction, i.e. $d=0$, then

$$\frac{C_{1m}}{C_{0m}}=1-\frac{p}{\lambda\beta_0^{\,2}}\left\{\frac{\Phi-1}{2\Phi^2}+\left(\frac{6\Phi-3\Phi^2-1}{4\Phi^4}\right)\frac{p}{\lambda\beta_0^{\,2}}\right\}+\cdots.$$

V. DISCHARGE FROM A MULTIPORT DIFFUSER

A standard of the modern engineering practice is to distribute and discharge the total effluent load over a series of ports by installing a multiport diffuser at the final section of the outfall pipeline, and thus in this case, each port discharging at a rate $q_0 = q_k = 1/(N+1)$.

By substituting $Y = 0$, we obtain from (3) for $X \ge -pN$, the compounded concentration of discharged effluents at the shoreline, in terms of the single outfall's concentration $C_{0-}(X,0)$, as

$$C_-(X,0) = C_{0-}(X,0)\left[q_0 + \sum_{k=1}^{N} q_k \sqrt{\frac{X}{X+kp}} \exp\left\{-\frac{\lambda\beta_k^{\ 2}}{4(X+kp)} + \frac{\lambda\beta_0^{\ 2}}{4X} - \gamma r^{\sigma} kp\right\}\right].$$

Substituting $X = X_{0m}$, and following the calculations as in the previous Section IV, the maximum value can be approximated as

$$\frac{C_{1m}}{C_{0m}} = q_0 + \sum_{k=1}^{N} q_k \exp\left(-\gamma r^{\sigma} kp\right)\sqrt{\frac{1}{1+kz}} \exp\left[-\frac{1}{2\Phi}\left\{\left(\frac{\beta_k}{\beta_0}\right)^2 \frac{1}{1+kz} - 1\right\}\right].$$

Since the value of γ is naturally small, $\beta_k = \beta_0 + kd/\sqrt{r}$ and the port's separation distances are relatively small, we obtain asymptotically

$$\frac{C_{Nm}}{C_{0m}} = \frac{1}{N+1} + \sum_{k=1}^{N} \frac{1}{N+1}\left[1 - \frac{1}{\Phi}\frac{d}{\beta_0\sqrt{r}}\left\{k + \left(\frac{\Phi-1}{2\Phi}\right)\frac{k^2 d}{\beta_0\sqrt{r}} - \frac{3}{2}k^2 z\right\} - \frac{z}{2\Phi}\left\{(\Phi-1)k + \left(\frac{3}{2} - \frac{3\Phi}{4} - \frac{1}{4\Phi}\right)k^2 z\right\} + \cdots\right],$$

and after summing for all N-ports,

$$\frac{C_{Nm}}{C_{0m}} = 1 - \frac{1}{2\Phi}\frac{d}{\beta_0\sqrt{r}}\left[N + \left\{\left(\frac{\Phi-1}{6\Phi}\right)\frac{d}{\beta_0\sqrt{r}} - \frac{z}{2}\right\}N(2N+1)\right] - z\left\{\left(\frac{\Phi-1}{4\Phi}\right)N + \left(\frac{6\Phi-3\Phi^2-1}{48\Phi^2}\right)zN(2N+1)\right\} + \cdots.$$

Thus, the maximum value of the compounded concentration of discharged effluents at the shoreline from a multiport diffuser C_{Nm} is less than that of the single outfall's C_{0m}. For the case of decay ($\gamma = 0$) effluents, then $\Phi = 1$ and

$$\frac{C_{Nm}}{C_{0m}} = 1 - \frac{d}{\beta_0\sqrt{r}}\left\{\frac{N}{2} - \frac{N(2N+1)}{2}\left(\frac{p}{\lambda\beta_0^{\ 2}}\right)\right\} - \frac{N(2N+1)}{6}\left(\frac{p}{\lambda\beta_0^{\ 2}}\right)^2 + \cdots.$$

If the multiport line diffuser with N-ports is installed in the y-axis perpendicular to the current direction (Figure 6 (left)), i.e. i.e. $p = 0$ or $z = 0$, then

$$\frac{C_{Nm}}{C_{0m}} = 1 - \frac{d}{\beta_0\sqrt{r}}\left[\frac{N}{2\Phi} + \left(\frac{\Phi-1}{12\Phi^2}\right)N(2N+1)\frac{d}{\beta_0\sqrt{r}}\right] + \cdots.$$

Similarly, if the multiport line diffuser with N-ports is installed in the x-axis parallel to the current direction, i.e. $d = 0$, then

$$\frac{C_{Nm}}{C_{0m}} = 1 - \frac{p}{\lambda\beta_0^{\ 2}}\left\{\left(\frac{\Phi-1}{2\Phi^2}\right)N + \left(\frac{6\Phi-3\Phi^2-1}{12\Phi^4}\right)N(2N+1)\frac{p}{\lambda\beta_0^{\ 2}}\right\} + \cdots.$$

Table -2 Ratio of maximum values C_{Nm}/C_{0m} for discharging no decay ($\gamma = 0$) effluents

N	2		4		6		8	
d	1.5	3	1.5	3	1.5	3	1.5	3
$r = 1$	0.9673	0.9345	0.9355	0.8710	0.9046	0.8095	0.8748	0.7498
$r = 1.5$	0.9727	0.9455	0.9463	0.8926	0.9206	0.8415	0.8958	0.7920
$r = 2$	0.9761	0.9522	0.9529	0.9059	0.9305	0.8611	0.9087	0.8179
$r = 2.5$	0.9784	0.9569	0.9575	0.9152	0.9373	0.8748	0.9177	0.8358
$r = 3$	0.9802	0.9604	0.9610	0.9221	0.9424	0.8850	0.9244	0.8493

As shown in Table 2, it is easy to see that as the number of ports N increases, and d gets longer, the maximum value of the compounded concentration at the shoreline C_{Nm} is smaller than that of the single outfall value C_{0m}. This result agrees with the standard engineering practice of installing a multiport diffuser at the end of the outfall pipeline to improve the mixing and dispersion of discharged effluents over the single outfall in coastal waters.

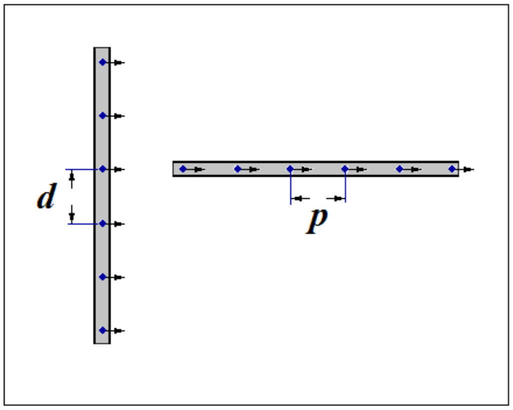

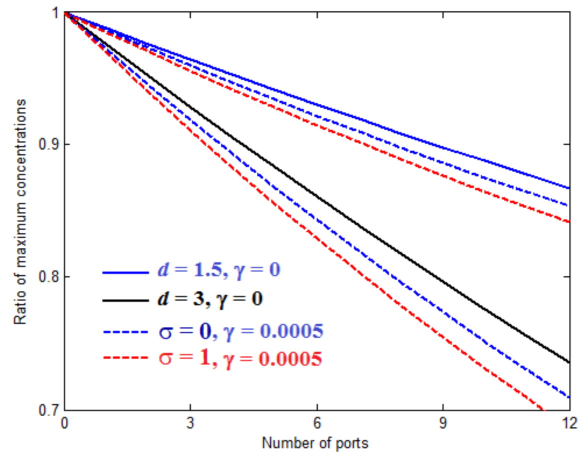

Figure 6 Special designs of multiport line diffuser (left), and the ratio of maximum concentration values C_{Nm}/C_{0m} for discharges from multiple point sources at $\alpha = 45$ on a step seabed for $\lambda = 0.2$ when $\ell = 40$ and $r = 2$ (right). The case of no decay $\gamma = 0$ with $d = p = 1.5$ (blue line) and with $d = 3$ and $p = 1.5$ (black line), constant decay of $\gamma = 0.0005$ and $\sigma = 0$ (dotted blue line), and decay of $\gamma = 0.0005$ that increases with depth $\sigma = 1$ (dotted red line)

Figure 6 (right) shows the ratio of maximum values C_{Nm}/C_{0m} as a function of the number of ports N for discharged effluents at $\alpha = 45$ on a step seabed or $\lambda = 0.2$ when $\ell = 40$ and $r = 2$ for two values of $d = 1.5$ and $d = 3$ with $p = 1.5$. Again, since the value of γ is naturally small, the effect of decay is too small to be noticeable. For example, for no decay ($\gamma = 0$) effluent discharges, if $d/\beta_0\sqrt{r} = 0.049$ (for $d = 3$) and $z = p/\lambda\beta_0^2 = 0.004$ (for $p = 1.5$), then the maximum value C_{Nm} is about 11.7% less than C_{0m} for $N = 5$ and is about 20.3% less for $N = 9$. For the case of effluents decay of $\gamma = 0.0005$ that increases with depth $\sigma = 1$, the additional reduction is about 2.8% for $N = 5$ and is about 4.2% for $N = 9$.

VI. CONCLUDING REMARKS

The human health risk from a sufficiently long and effectively well design sea outfall effluents discharge is generally considered low. Analytical solutions of a two-dimensional decay-advection-diffusion equation with multiple point sources on a step seabed depth profile are used to study the mixing and dispersion of chemically active discharged effluent plumes from a multiport diffuser in the far field. The variability of decay of discharged effluents with water depth is accounted for in the solutions, and the results show that the extent of downstream mixing is less than that of no-decay discharged effluents. Diffuser-induced concentration at the shoreline is then formulated, and based on the maximum values, it is found that positioning the diffuser line perpendicular to the current direction enhances the spreading of discharged effluent plumes. The effectiveness of multiport diffusers for discharging effluents on a step seabed depth is slightly reduced compared to that of a flat seabed. This is mainly due to the shallow nearshore region that acts like a trap to delay and restrain dilution of the discharged effluents.

VII. ACKNOWLEDGEMENT

This work was supported by the Sultan Qaboos University Internal Grant IG/SCI/DOMS/18/04.

VIII. REFERENCES

[1] Institution of Civil Engineers, "Long Sea Outfalls". 1st ed., Thomas Telford Ltd., London, 2001.

[2] P.J.W. Roberts, H.J. Salas, F.M. Reiff, M. Libhaber, A. Labbe and J.C. Thomson, "Marine Wastewater Outfalls and Treatment Systems". International Water Association (IWA) Publishing, London, 2010.

[3] J.F. Macqueen and R.W. Preston, "Cooling water discharges into a sea with a sloping bed", Water Research, vol. 17 (1983) 389-395.

[4] N. Ahmad and R.E. Baddour, "A review of sources, effects, disposal methods, and regulations of brine into marine environments", Ocean and Coastal Management, vol. 87 (2014) 1-7.

[5] D.J. Gould and D. Munro, "Relevance of microbial mortality to outfall design", in Coastal Discharges – Engineering Aspect and Experience, Thomas Telford, Ltd., London, 1981.
[6] G.H. Jirka, "Integral model of turbulent buoyant jets in unbounded stratified flows. Part 2. Plane jet dynamics resulting from multiport diffuser jets", Environmental Fluid Dynamics, vol. 6 (2006) 43-100.
[7] A. Purnama, H.H. Al-Barwani, T. Bleninger and R.L. Doneker, "CORMIX simulations of brine discharges from Barka plants, Oman", Desalination and Water Treatment, vol. 32 (2011) 329-338.
[8] D.A. Roberts, E.L. Johnston and N.A. Knott, "Impacts of desalination plants discharges on the marine environment: A critical review of published studies", Water Research, vol. 44 (2010) 5117-5128.
[9] A. Purnama, H.H. Al-Barwani, M.S. Al-Rawahi and T.M. Al-Harthi, "Dispersion models for brine discharges from desalination plants of Oman", Kuwait Journal of Science and Engineering, vol. 31 (2004) 1-13.
[10] R. Smith, "Effects of non-uniform currents and depth variations upon steady discharges in shallow water", Journal of Fluid Mechanics, vol. 110 (1981) 373-380.
[11] A. Kay, "The effect of cross-stream depth variations upon contaminant dispersion in a vertically well-mixed current", Estuarine and Coastal Shelf Science, vol. 24 (1987) 177-204.
[12] M.L. Yates, R.T. Guza and W.C. O'Reilly, "Equilibrium shoreline response: Observations and modelling", Journal of Geophysical Research, vol. 114 (2009) C09014.
[13] P. Dissanayake, J. Brown and H. Karunarathna, "Impacts of storm chronology on the morphological changes of the Formby beach and dune system", UK, Natural Hazards and Earth System Sciences, vol. 15 (2015) 1533-1543.
[14] A.M. Bernabeu, R. Medina and C. Vidal, "Wave reflection on natural beaches: an equilibrium profile model", Estuarine, Coastal and Shelf Science, vol. 57 (2003) 577-585.
[15] R.G. Dean, "Equilibrium beach profile: Characteristics and applications", Journal of Coastal Research, vol. 7 (1991) 53-84.
[16] D.A. Chin and P.J.W. Roberts, "Model of dispersion in coastal waters", Journal of Hydraulic Engineering, vol. 111 (1985) 12-28.
[17] I.R. Wood, "Asymptotic solutions and behavior of outfall plumes", Journal of Hydraulic Engineering, vol. 119 (1993) 553-580.
[18] H.H. Al-Barwani and A. Purnama, "Simulating brine plumes discharged into the seawaters", Desalination, vol. 221 (2008) 608-613.
[19] A. Purnama and D.D. Shao, "Modeling brine discharge dispersion from two adjacent desalination outfalls in coastal waters", Desalination, vol. 362 (2015) 68-73.
[20] D.L. Craig, H.J. Fallowfield and N.J. Cromar, "Comparison of decay rates of faecal indicator organisms in recreational coastal water and sediment", Water Supply, vol. 2 (2002), 131-138.
[21] A. Adcroft, R. Hallberg, J.P. Dunne, B.L. Samuels and J.A. Galt, "Simulations of underwater plumes of dissolved oil in the Gulf of Mexico", Geophysical Research Letters, vol. 37 (2010), L18605.
[22] V.P. Shukla, "Analytical solutions for unsteady transport dispersion of nonconservative pollutant with time-dependent periodic waste discharge concentration", Journal of Hydraulic Engineering, vol. 128 (2002), 866-869.
[23] D.W. Ostendorf, "Longshore dispersion over a flat beach", Journal of Geophysical Research, vol. 87 (1982) 4241-4248.
[24] R. Smith, "Longitudinal dispersion of buoyant contaminant in a shallow channel", Journal of Fluid Mechanics, vol. 78 (1976) 677-688.
[25] P. Mebine and R. Smith, "Effects of contaminant decay on the diffusion centre of a river", Environmental Fluid Mechanics, vol. 6 (2006), 101-114.
[26] P. Mebine and R. Smith, "Effect of pollutant decay on steady-state concentration distributions in variable depth flow", Environmental Fluid Mechanics, vol. 9 (2009), 573-586.
[27] R. Smith and A. Purnama, "Two outfalls in an estuary: Optimal wasteload allocation", Journal of Engineering Mathematics, vol. 35 (1999), 273-283.
[28] A. Purnama, "Effluent discharges from two outfalls on a sloping beach", Applied Mathematics, vol. 5 (2014), 3117-3126.